Article

A CD44-biosensor for evaluating metastatic potential of breast cancer cells based on quartz crystal microbalance

Xiaojuan Yang, Rongcheng Zhou, Yan Hao, Peihui Yang

PII: S2095-9273(17)30283-9
DOI: http://dx.doi.org/10.1016/j.scib.2017.05.022
Reference: SCIB 149

To appear in: *Science Bulletin*

Received Date: 19 March 2017
Revised Date: 20 April 2017
Accepted Date: 26 April 2017

Please cite this article as: X. Yang, R. Zhou, Y. Hao, P. Yang, A CD44-biosensor for evaluating metastatic potential of breast cancer cells based on quartz crystal microbalance, *Science Bulletin* (2017), doi: http://dx.doi.org/10.1016/j.scib.2017.05.022

Article

Received 19 March, 2017

Revised 20 April, 2017

Accepted 26April, 2017

A CD44-biosensor for evaluating metastatic potential of breast cancer cells based on quartz crystal microbalance

Xiaojuan Yang，Rongcheng Zhou，Yan Hao，Peihui Yang*

Department of Chemistry, Jinan University, Guangzhou 510632, China

Corresponding author: E-mail: typh@jnu.edu.cn

Tel/Fax: +86-20-85223039

Xiaojuan Yang E-mail: ouyangxj@yahoo.com

Abstract A sensitive CD44-biosensor based on quartz crystal microbalance (QCM) was proposed for evaluating metastatic potential of breast cancer cells by using hyaluronan (HA) functionalized substrate film, polydopamine and polyethyleneimine composite film, for the purpose of capturing CD44-positive cancer cells through specific binding of HA to CD44. Two differently CD44-expressed breast cancer cell lines (MDA-MB-231 cells and MCF-7 cells) were put to use as targets for quantitative analysis as well as evaluation of metastatic potential of the cells. The limit of detection for MDA-MB-231 (M231) cells and MCF-7 cells were 300 and 1,000 cells mL^{-1}, respectively. The expression level of CD44 on M231 cells exhibited two times higher than that of MCF-7 cells, indicating of a higher metastatic potential. Moreover, poly-L-lysine modified QCM sensor was applied to monitor the stiffness of breast cancer cells that can reflect metastatic potential of cells. The results revealed that the

MCF-7 cells were stiffer than M231 cells, implying that the M231 cells possessed higher metastatic potential. The proposed protocol is simple and rapid to evaluate the metastatic potential of cancer cells, in addition to offering a promising diagnostic tool for metastatic cancer.

Keywords CD44 · Quartz crystal microbalance · Metastatic potential · Breast cancer cells · Stiffness

1 Introduction

Metastatic potential of cancer cells plays a crucial role in cancer metastasis, which is the main cause of cancer treatment failure and patients' deaths [1,2]. Detection and characterization of metastatic cancer cells are vital in both cancer diagnose and treatment [3]. Conventional approaches have been used for the diagnosis of malignant cancer, for instance tissue's morphological, immunohistochemical assay and radiological method. However, they are time consuming with complicated sample preparation and are radiohazard. It is reported that the metastatic potential of cancer cells is usually associated with the abnormalities of biological and mechanical properties of cancer cells, such as cell deformability, stiffness, viscoelasticity [4,5]. Therefore, new methods for analysis of biophysical properties of cells are quite considerable in order to give insight into their roles in cancer progression.

Recent advances in methodologies such as atomic force microscopy (AFM) [6,7], Raman spectroscopy [8], electrical spectroscopy [9], microfluidic [10, 11] and fluorescence methods [12,13], on basis of measurement variation of biomolecule or mechanical properties for the purpose of probing into metastatic potential of cancer cells, have driven it possible to provide new diagnostic approaches. But, these techniques usually required well-trained personnel and chromophores/fluorophores tagging and expensive equipment. Therefore, it is necessary to develop novel assays that would be easily applicable for label-free evaluation of metastatic cancer cells. Quartz crystal microbalance (QCM), being a new sensitive mass sensor, has become an attractive analytical tool because of its unique advantages like high sensitivity, facile operation and label-free and real-time detection [14-16]. QCM takes the measurements of changes in mass near the sensor surface as a shift in the resonance frequency (f) of the

sensor crystal. In addition, the sensor oscillation decay rate delivers information about dissipative energy losses (D) that possesses relation with viscoelastic properties of the deposited layers. Equally important, combined dissipation and frequency shift (ΔD-Δf) measurement, i.e., the change in measured energy dissipation per surface-coupled unit mass, is capable of being put to use for the purpose of extracting information related to the structural properties of the adsorbed layers [17,18]. QCM has been widely applied in bioassays including detection of protein [19,20], nucleic acids [21], cells [22] and carbohydrates [23]. Moreover, mechanical properties of the cells can be monitored by QCM as well, such as cytoskeletal [24,25], motility [26], and stiffness [27]. Recently, Atay et al. [28] proposed a transferrin modified QCM for detecting highly metastatic breast cancer cells. Sobiepanek et al. [29] used QCM for distinction of melanoma cells with a different metastatic potential by monitoring lectin-carbohydrate interaction. Zhou et al. [25] described a QCM sensor for dynamic monitoring viscoelastic index of cancer cell and normal cell during adhesion process. Tarantola et al. [26] reported a QCM sensor for assaying cell motility of human cancer cells. As is reported, QCM biosensors exhibited excellent analytical performance for the measurement of cell function. However, to the best of our knowledge, no reports concerning the investigation of metastatic potential of cancer cells via measurement of biomolecule expression level and mechanical properties of cells by QCM. It is still worthy to develop some simple, facile and sensitive QCM strategies for the evaluation of the metastatic potential of cells taking into consideration the bases of the detection of multiple markers of cancer cells.

CD44, which is a family of adhesion molecules, involved in various biological functions, for example cell proliferation, division and migration [30,31].The CD44 expression level play important roles in cancer metastasis, and higher expression of CD44 is expressed on high metastatic cancer cells surface as compared with their less metastatic counterparts [32,33]. Basakran [34] deemed that monitoring changes in CD44 level on cancer cells surface can serve as a specific and sensitive cancer marker. Hyaluronan (HA), ligand of CD44, a biocompatible and negatively charged glycosaminoglycan, has been widely investigated for specific targeting of CD44 over-expressed cancer cells [30,35]. Additionally, dopamine, a kind of mussel adhesive proteins, has also attracted great amount of attention in the surface

chemistry due to its outstanding ability to bind strongly to almost all kinds of objects, in addition to providing secondary reactivity for anchoring molecules with amine or sulfhydryl group in order to create a variety of ad-layers by self-polymerization on substrate surface [36], so that it was selected as an ideal immobilized material in QCM aimed at enhancing the stability and activity of the biosensor. Polyethyleneimine (PEI), rich in amine groups, was adopted to covalently graft onto the polydopamine (PDA) layer to fabricate a positively charged membrane and bind HA via electrostatic interactions. Thus, HA molecules could be stoutly attached to gold chip through PDA/PEI film functioning as an adhesive first layer and promoting the robust anchorage of CD44 over-expressed cancer cells onto the sensor interface.

Herein, we present a simple QCM-based CD44 biosensor for evaluating metastatic potential of breast cancer cells by assessing the CD44 expression and the stiffness of cancer cells. HA functionalized PDA/PEI composite film (PDA/PEI/HA) was modified on the gold chip to capture breast cancer cells via specific recognition of the CD44 on cell surface that provided an optimal high selectivity and stability sensing interface for the detection of two types CD44-positive breast cancer cells. It was further applied for the evaluation of the metastatic potential of cancer cells. Additionally, the metastatic potential of the breast cancer cells was characterized by the stiffness of cells that was monitored by PLL-modified QCM sensor. The proposed biosensor provided a promising protocol for a sensitive as well as evaluation of cancerous stages.

2 Experimental

2.1 Reagents and apparatus

Human breast cancer cell lines MDA-MB-231 (M231) and MCF-7 were donated by Institute of Physiology, Jinan University (China). Dopamine hydrochloride and polyethyleneimine (PEI, M_w=10,000) were products of Aladdin. Co. Sodium hyaluronate (HA) with a molecular weight of 0.8×10^6–2.0×10^6 was obtained from QiYun Biological Technology Co. Ltd. (Guangzhou, China). Poly-L-lysine (PLL, M_w≥300,000) and 4% paraformaldehyde were products of Biosharp, China. All

reagents were of analytical grade. Ultrapure water was used throughout the study. Quartz crystals (5 MHz) in the form of 14 mm disks with a gold electrode (10 mm diameter) formed uniformly on one side were used. Resonant frequency and energy dissipation factor recorded using the QCM sensor (KSV QCMZ500, Q-Sense Co., Sweden). Data analysis was performed using QcmZBrwse software from Q-Sense. Cyclic voltammetry (*CV*) was performed on CHI660D electrochemistry workstation (CH Instruments Co., USA). The working electrode either the untreated or modified Au electrode, a saturated calomel electrode being the reference electrode and platinum wire were used as the auxiliary electrode. Contact angle measurements were performed with contact angle meter (JC2000C2, ZhongChen digital technology Co., Ltd. China). Morphology of the biosensor surfaces was visually characterized by scanning electron microscopy (SEM, JEOL-JSM-6700F, Philips Electron Optics, Netherland,). Fluorescent images were taken by using the Nikon inverted microscope (ECLIPSE TE-2000U, Nikon, Japan).

2.2 Cell culture

M231 cells and MCF-7 cells were grown in RPMI 1640 (Gibco Co., China) culture media supplemented with streptomycin (100 U mL^{-1}), penicillin (100 U mL^{-1}), and fetal bovine serum (10%) in an incubator (5% CO_2, 37 °C). At the logarithmic phase, the cells were collected by centrifugation at 800 r min^{-1} for 5 min, following a wash with phosphate buffered saline (PBS), and re-dispersed in sterile PBS for further utilization.

2.3 Synthesis of PDA/PEI/HA film

Robust and specific composite film was fabricated to modified QCM gold chip (Au chip). PEI, as covalently conjugated with PDA, was selected as a support platform for the modification of HA (Fig. 1a). The formed PDA/PEI/HA film could specific binding CD44-positive breast cancer cells. Briefly, 4 mg mL^{-1} dopamine was prepared by dissolving dopamine hydrochloride in Tris buffer solution (pH 8.5, 50 mmol L^{-1}) and PDA coatings through simple dip-coating of substrates in above-mentioned dopamine solution [39]. After deposition, samples were cleaned

using the deionized water. Thereafter, the objects were dipped into the PEI solutions for a period of 1 h, and labeled as PDA/PEI film. Following it, negatively-charged HA (0.5 mg mL^{-1}) coating was formed through electrostatically-driven assembly.

2.4 Cancer cells metastasis analysis procedure

Prior to modification, Au chips were cleaned by dipping them in piranha solution (H_2SO_4:H_2O_2 = 3:1, v/v) for 10 min to remove impurities. Later on, they were rinsed thoroughly with deionized water and dried by nitrogen gas before to use. Schematic diagram of the CD44 biosensor construction was showed in Fig. 1b. After obtaining PDA/PEI/HA composite film coated Au chip, the modified chips were mounted in a flow chamber, and the PBS assay buffer followed first. After obtaining stable baselines in liquid condition, the flow fluid was replaced by different cancer cells. After that, rinsing with PBS buffer solution was done in order to remove non-bound samples in the end. In respect of the stiffness assay of the cancer cells, the modified chips were prepared according to a published procedure [17]. The measurement procedures of the cells mechanical were similar to the cell recognition assay mentioned above.

2.5 AFM measurements

Morphological imaging and mechanical properties of cells were carried out by using the BioScope Catalyst (Bruker, Germany) AFM system. The AFM probes were Tap 150Al-G Silicon probes, which were purchased from Budget Sensors Company (Bulgaria). The material properties and dimensions of the AFM tips used in this experiment were as follows: force constant of 0.7110–1.089 Nm^{-1} (Nom. 1.089 Nm^{-1}), tip height of 17 μm (±2 μm), cantilever width of 5 μm (±2 μm), resonance frequency of 40–75 kHz, cantilever thickness of 0.6 μm (±0.05 μm), tip radius of 10 nm (±2 nm) and cantilever length of 120 μm (±5 μm). For the imaging of M231 cells and MCF-7 cells, the cells were fixed by paraformaldehyde for 10 min, following imaging in air at 256×256 pixels resolution and 0.7110 Hz scan speed at room temperature. The scan area was depended on the size of the cancer cells. The ultrastructural parameters to

evaluate cell's surface roughness were arithmetic average roughness (R_a) and root-mean-square roughness (R_q) by calculating 20 different ultrastructure areas (3 μm×3 μm, selected randomly). Yang modulus was performed in the Force Volume mode under the same conditions whereby every set of measurement was performed more than five different locations on five different cells. Measurement of the force curves was taken more than 1,000 times for each treated cell.

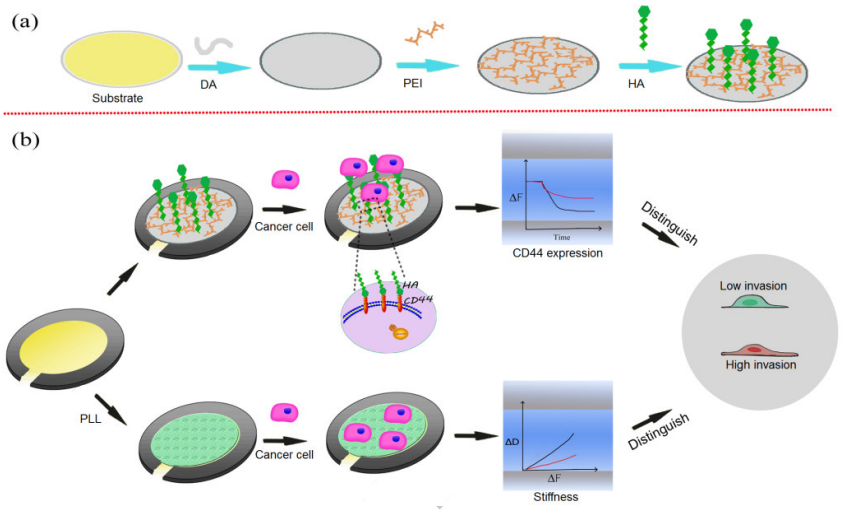

Fig. 1 (Color online) (a) Synthesis of PDA/PEI/HA film. (b) Schematic illustration of the CD44 biosensor based QCM for evaluating metastatic potential of breast cancer cells

3 Results and discussion

3.1 Characterization of CD44-biosensor interface

HA-functionalized PADA/PEI composite film was modified on Au chip and was used to capture breast cancer cells via specific recognition of the CD44 on cell surface. *CV* and QCM were employed to monitor the fabricate process of PDA/PEI/HA film. As shown in Fig. 2a, one pair of well-defined redox peaks originated from electrochemical probe $[Fe(CN)_6]^{3-/4-}$ was observed on bare Au chip. After deposition of PDA, the redox peak almost disappeared, revealing that the electron transfer capacity was degraded. It was ascribed to oxidation and reduction of the dopamine/dopaminequinone in the film [37]. When the PEI was immobilized bound onto the above chip surface via Schiff base reactions or Michael addition, the intensity

of both the cathodic and anodic peak current profiled the redox peak increase. This phenomenon was attributed to the PEI with plentiful positive charges that were favorable for the electron transfer between the $[Fe(CN)_6]^{3-/4-}$ and chip surface as a result of electrostatic attraction. The PDA/PEI composite film was modified with HA, an obvious decrease in the peak current was observed due to its surface being negatively charged and the repulsion to the signal probe towards the electrode surface, confirming the successful assembly of the biosensor. QCM was further used to verify the assemble processes of the modified sensor. As shown in Fig. 2b, the frequency was successively decreased following the step by step grafting of PEI and HA onto the PDA-coated chip surface, indicating the successful binding of PEI and HA to the PDA modified Au chip. Furthermore, as shown in Fig. 2c, the frequency response of HA absorbed on the PEI/PDA-modified QCM sensor (curve c) was 3 times greater than the PDA-modified one (curve b). This phenomenon was ascribed to the existence of PEI increasing the HA absorption on QCM sensor surface, because of the electrostatic interaction between negatively charged HA and positively charged PEI. Interestingly, when the HA was immobilized onto the bare Au chip, a negligible frequency decrease was observed (Fig. 2c, curve a). This might be because of the Au surface lacking functional groups to trap HA molecule, leading to low frequency response. These results demonstrated that the introduction of PEI could effectively enhance the loading amount of the HA on biosensor interface thus offering a more sensitive surface for capturing CD44-positive cancer cells.

The hydrophilicity of composite film was characterized by measurement of the contact angle. As seen in Fig. 2d, contact angles for bare Au, PDA, PDA/PEI and PDA/PEI/HA film were 67°, 59°, 32° and 24°, respectively. Because of the relatively hydrophilic functional groups (amines, carboxyl, and phenol hydroxyl groups) of PEI and HA, the water contact angle decreased to 24° following the HA coating formation. The result suggested that the designed PDA/PEI/HA film could provide a biocompatible biosensor interface.

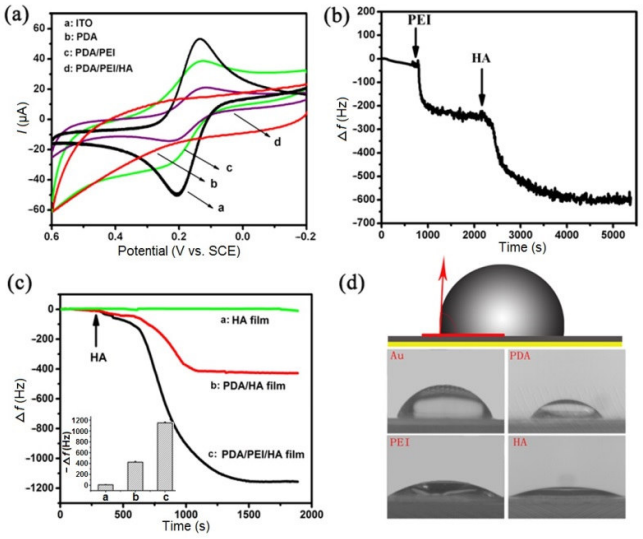

Fig. 2 (Color online) Characterization of CD44-biosensor interface. (a) *CV*; (b), (c) real-time frequency response of the QCM to the layer-by-layer assembly of PDA/PEI/HA film; (d) contact angle

The surface morphology of the biosensor surface was visualized by SEM. As shown in Fig. 3, the unmodified substrate had a smooth and clear surface (Fig. 3a), while the PDA-modified substrate displayed several surface pores (Fig. 3b). After PEI grafting, the membrane surface showed a layer of porous films, possibly because of grafting of PEI molecules, whose chains were rather flexible [38]. Eterogeneity and microsized aggregates of the membrane surface were observed after HA adsorption. The above results indicated that the coating film had been successfully assembled.

Fluorescence microscopy was used to characterize the biosensor for capturing of different breast cancer cells, M231 cells and MCF-7 cells, stained by FITC, respectively. As shown in Fig. 3e and f, two types of breast cancer cells could be observed on the composite film interfaces, while the captured number of M231 cells was obviously more than MCF-7 cells, suggesting the excellent selectivity of the biosensor for CD44-overexpressing cancer cells.

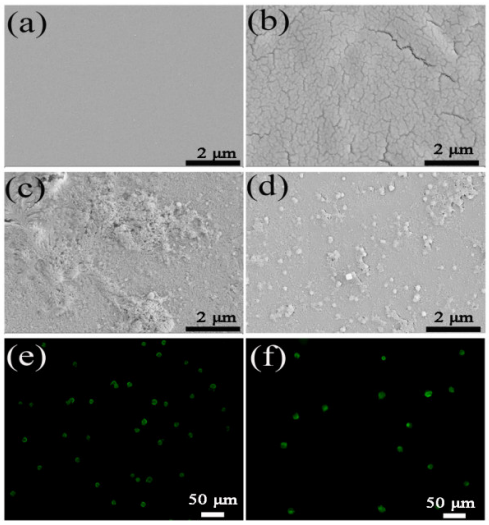

Fig. 3 (Color online) SEM images of the biosensor surface. (a) Substrate, (b) PDA film, (c) PDA/PEI film, and (d) PDA/PEI/HA composite film. Fluorescence microscopy images for breast cancer cells captured by PDA/PEI/HA film coated surface: (e) M231 cells and (f) MCF-7 cells

3.2 Detection of breast cancer cells by CD44-biosensor

Breast cancer cells were quantitatively detected by using the proposed biosensor for the evaluation of the sensitivity and quantitative range. As shown in Fig. 4a, the frequency response increased with the increment of the M231 cells concentration, and it was linear with the logarithm of the concentration of M231 cells in the range from 1×10^3 to 5.0×10^5 cells mL^{-1} with a limit of detection (LOD) of 300 cells mL^{-1}. The biosensor was further used for the detection of MCF-7 cells and showed a linear response towards the logarithm of the concentration of MCF-7 cells ranging from 5×10^3 to 4×10^5 cells mL^{-1} with a LOD of 1,000 cells mL^{-1} (Fig. 4b). Therefore, the sensitivity of the assay was comparably sensitive with other QCM biosensor such as aptamer-based QCM biosensor for detection of leukemia cells [22].

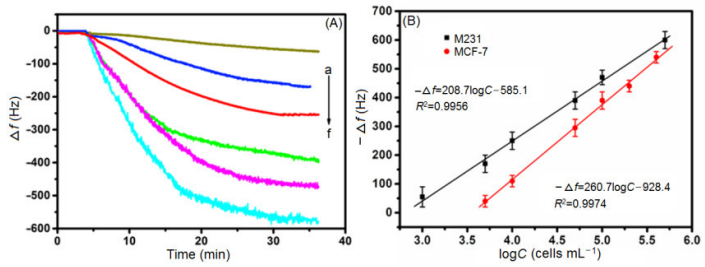

Fig. 4 (Color online) (A) Real-time frequency responses of the CD44-biosensor with different concentrations of M231 cells: a–f: 1×10^3, 5×10^3, 1×10^4, 5×10^4, 1×10^5, 5×10^5 cells mL^{-1}, respectively. (B) Plots of QCM frequency intensities vs. logarithm value of MCF-7 cells and M231 cell concentration (cells mL^{-1})

3.3 Selectivity of the biosensor

The selectivity of the proposed biosensor was investigated by a comparison of the QCM responses of different CD44-expression cell lines with the same concentration, including M231 cells, MCF-7 cells, erythrocytes and endothelial cells (HUVECs), respectively. As shown in Fig. 5, remarkable frequency signal changes were observed for M231 cells and MCF-7 cells (c and e), whereas minimal frequency signal changes were observed for erythrocytes and HUVECs (a and b). Moreover, the mixed sample (M231 cells or MCF-7 cells coexisting with HUVECs) did not show a clear change compared with that of M231 cells or MCF-7 cells solely. These results demonstrated that the CD44-biosensor is highly specific and selective for CD44-overexpression cells.

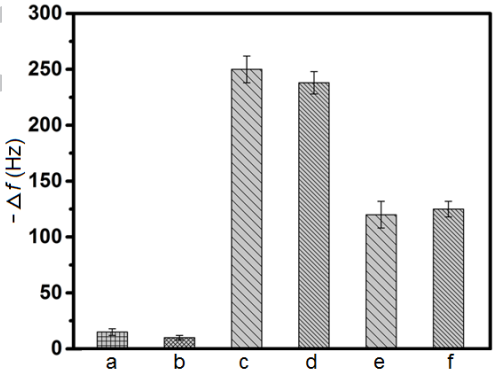

Fig. 5 Specificity and selectivity of the PDA/PEI/HA film modified QCM biosensor for

different cell lines at a concentration of 1.0×10^4 cells mL^{-1}. (a) Erythrocytes, (b) HUVECs, (c) M231 cells, (d) mixture of HUVECs and M231 cells, (e) MCF-7 cells, and (f) mixture of HUVECs and MCF-7 cells

3.4 Evaluating metastatic potential of breast cancer cells by CD44-biosensor

The CD44-biosensor was further applied to evaluate the metastatic potential of breast cancer cells. The CD44 expression level of the cancer cells, having a strong correlation with its cancerous state, could be derived from the frequency signals measured by QCM. Frequency responses of the proposed biosensor for two different cell lines were shown in Fig. 6. Note that the very different and readily distinguishable Δf signal of two cells types were observed, taken into notice whereby the Δf signal of M231 cells larger approximately 2-fold than MCF-7 cells, suggesting that higher amount of M231 cells were captured onto the biosensor surface. Furthermore, blocking experiments were performed by using free HA to block recognition site on cancer cells surface (Fig. 6a, curve c and d). The result showed that the Δf had dramatically decreased to ~40 and ~20 Hz for M231 cells and MCF-7 cells, respectively, indicating the abolishment of the recognition spots between HA and CD44 on cell surface leading to fewer breast cancer cells captured by the CD44-biosensor. These results demonstrated that the M231 cells possessed higher metastatic potential and the method proposed could be used for distinction of breast cancer cells with different metastatic potential.

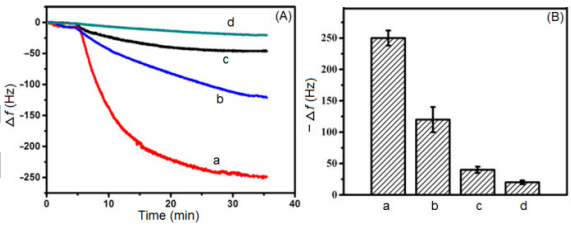

Fig. 6 (Color online) (A) Real-time frequency response of the CD44-biosensor to the additions of 1×10^4 (cells mL^{-1}) cells: (a) M231 cells, (b) MCF-7 cells, (c) M231 cells incubation with free HA, and (d) MCF-7 cells incubation with free HA, respectively. (B) Normalized frequency responses of the QCM biosensor with different cells lines

3.5 Wound-healing assay

Wound-healing assay was carried out to explore motility of M231 and MCF-7 cells in vitro that is the classical assays for migration and invasion of cancer cells. Wounds were made by using pipette tip and photographs were taken immediately 12 or 24 h after wounding for cancer cells. The distance migrated by the cells monolayer to close the wounded area was measured (Fig. 7). At 24 h, the migration index of the MCF-7 cancer cells and M231 cells were 94.19%±0.61%, 54.35%±2.99%, respectively. The result indicated that cells migrated more quickly to close the scratched wounds of M231 compared with MCF-7 cancer cells, further suggesting that M231 cells had stronger metastatic potential.

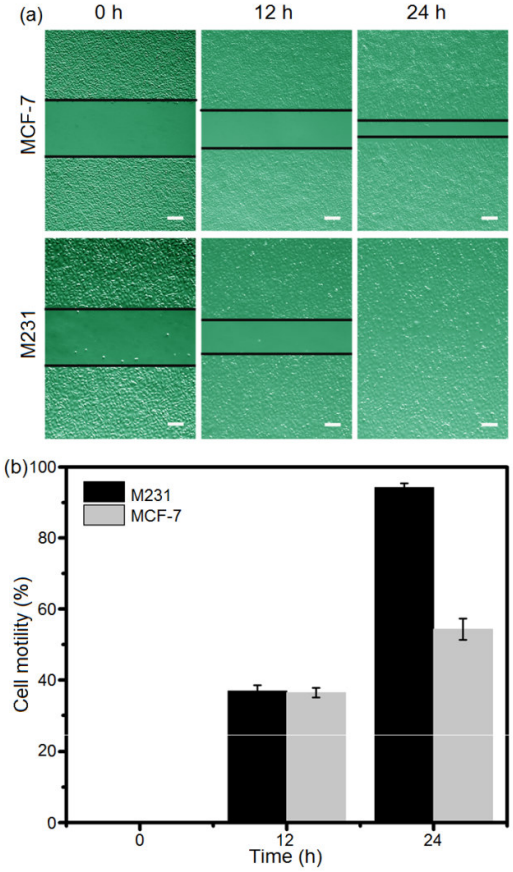

Fig. 7 (Color online) (a) Representative pictures of the wound-healing assay for cells migration. (b) The cell motility was quantitatively analyzed. Scare bar: 100 μm

3.6 Characterized stiffness of the M231 and MCF-7 cells by QCM

During the cell's transition of from normal state to immortal cancerous cell, the cytoskeleton devolves from a rather rigid structure to a more compliant state, which in turn induces changes in cell stiffness [4]. Therefore, relationship between the stiffness and the potential for migration of breast cancer cells was studied by QCM. PLL-modified QCM sensor was used for detecting the cell stiffness by simultaneously monitoring dissipation and frequency. As shown in Fig. 8, decreasing frequency and increasing dissipation were observed both the MCF-7 cells and M231 cells. However, the slope $|\Delta D/\Delta f|$ for MCF-7 cells (0.05) was lower than that for M231 cells (0.15), indicating that the MCF-7 cells were stiffer while displaying decreased deformation. The plasma membrane of high metastasis breast cancer cells possessed less rigidity owed to the lower polarization and limiting anisotropy. These results revealed that the ΔD-Δf parameters are useful towards characterizing stiffness of cells to evaluate metastatic potential of cancer cells.

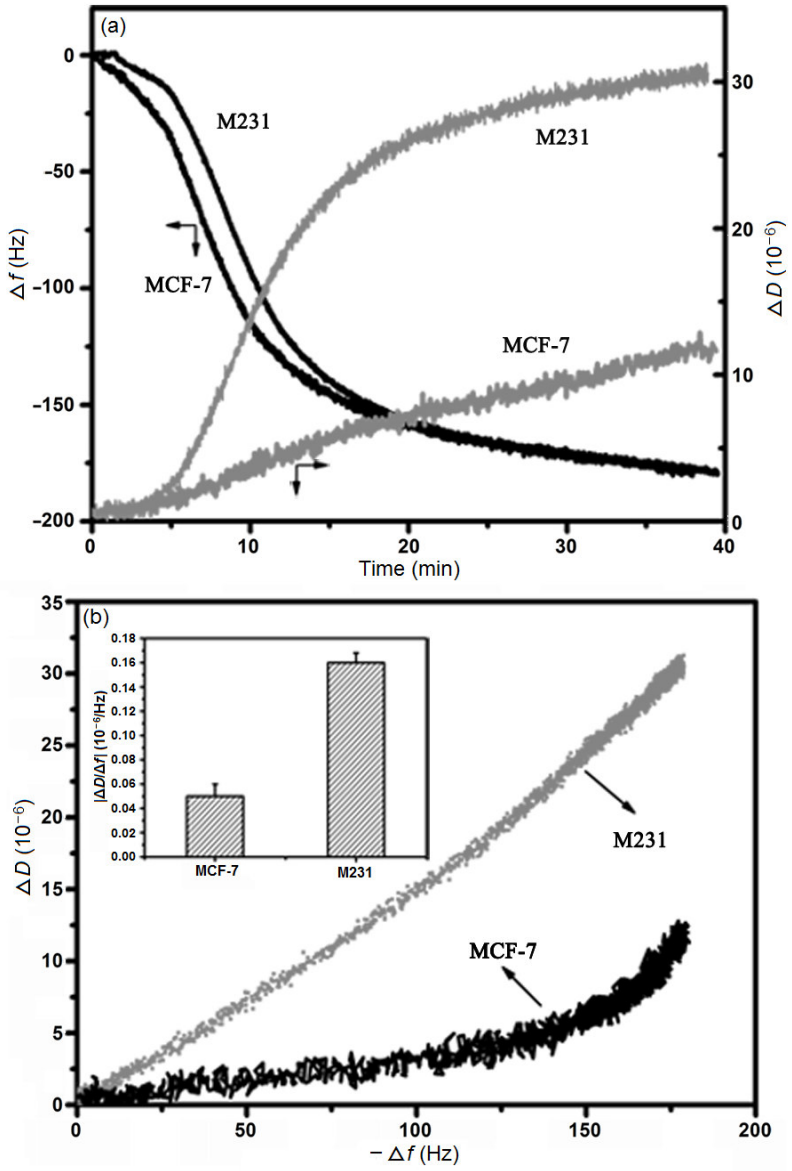

Fig. 8 (a) Real-time frequency and dissipation factor responses of the PLL-modified QCM sensor for the M231 cells and MCF-7 cells (4,000 cell mL^{-1}). (b) The average plot of ΔD-Δf results of MCF-7 cells and M231 cells measured by QCM sensor. Insert: the histogram of $|\Delta D/\Delta f|$ plots

3.7 AFM observations for surface morphology and stiffness of cancer cells

AFM was used to investigate the morphology, ultrastructure and stiffness of breast cancer cells. Fig. 9a and d showed the morphology of two types of cancer cells. It was obviously observed that both M231 cells and MCF-7 cells revealed long-spindle shaped morphology and

pseudopodium. The cell membrane was smooth and intact. Moreover, as Young's modulus was the evaluation indicator of cell stiffness, which was shown in Fig. 9b and e, the value was 22.56±1.50 kPa and 34.99±4.91 kPa for M231 and MCF-7, respectively. The result revealed the negative correlation between the stiffness of the cell and cell metastasis. This may be attributed to the reduction in the amount of well-organized filamentous actin or stress fibers that directly contribute to cell elasticity and hence malignant cell is likely to possess the stronger potential to migrate through surrounding tissue matrix and small capillaries [5]. Moreover, as shown in Fig. 9f, the surface roughness was used to study the difference of the cancer cells morphology quantitatively. Both R_a and R_q of M231 cells were much bigger as compared with MCF-7 cells, indicating that the membrane of M231 cells was rougher than the MCF-7 cells, which might be attributed to over-expression of some membrane protein. These results showed good consistency with the results achieved from QCM, implying that the QCM technique can sensitively measure changes in cell stiffness.

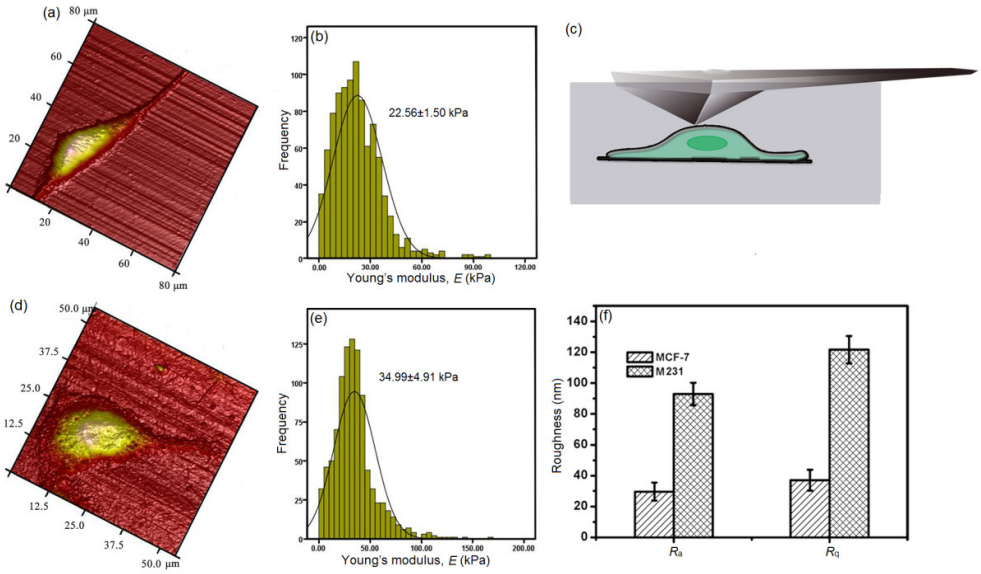

Fig. 9 (Color online) AFM measurement of different breast cancer cell lines. AFM morphology of M231 cell (a) and MCF-7 cell (d); Young's modulus of M231 cells (b) and MCF-7 cells (n=20) (e); (c) schematic diagram of AFM measurement; (f) ultrastructural properties of M231 cells and MCF-7 cells

3.8 Stability and reproducibility of CD44-biosensor

The stability and reproducibility of the protocol is of great importance to appraise sensor feasibility. The PDA/PEI/HA modified Au chip retained its QCM response without obvious decline after a week at 4 ℃ that suggested that the CD44-biosensor was efficient enough to hold its stability. Evaluation of the reproducibility of the biosensor was performed by determining the same concentration of cancer cells with three biosensors of different batches under the same experiment conditions. The relative standard deviation of the inter-assay was 4.23% at the M231 concentration of 1×10^5 cells mL^{-1}, indicating an acceptable precision and reproducibility.

4 Conclusion

A facile QCM-based CD44-biosensor was fabricated for distinguishing the metastasis potential of breast cancer cells by evaluating the CD44 expression and the stiffness of cells. The PDA/PEI/HA composite film modified biosensor exhibited desirable performance for quantitative detection of the CD44-possitive cancer cells. Larger changes in frequency indicated the higher metastasis cancer cells directly. Moreover, during the processes of cancer cells adhesion to the sensor surface, the stiffness being associated with the metastatic potential of the cancer cells, was measured by QCM. The results collectively showed that this protocol could be a suitable candidate for distinguishing metastatic potential of cancer cells with considerable specificity and high precision. Also, it would be beneficial to the understanding of mechanism of the tumor development and metastasis.

Acknowledgments This work was supported by the National Natural Science Foundation of China (21375048).

Conflict of interest The authors declare that they have no conflict of interest.

References

1. Siegel R, Ma J, Zou Z et al (2014) Cancer statistics, 2014. CA Cancer J Clin 64: 9-29

2. Gassmann P, Haier J (2008) The tumor cell-host organ interface in the early onset of metastatic organ colonisation. Clin Exp Metastasis 25: 171-181

3. Senkus E, Cardoso F, Pagani O (2014) Time for more optimism in metastatic breast cancer? Cancer Treat Rev 40: 220-228

4. Xu W, Mezencev R, Kim B et al (2012) Cell stiffness is a biomarker of the metastatic potential of ovarian cancer cells. PLoS One 7: e46609

5. Swaminathan V, Mythreye K, O'Brien ET et al (2011) Mechanical stiffness grades metastatic potential in patient tumor cells and in cancer cell lines. Cancer Res 71: 5075-5080

6. Li QS, Lee GY, Ong CN et al (2008) AFM indentation study of breast cancer cells. Biochem Biophys Res Commun 374: 609-613

7. Barbieux C, Bacharouche J, Soussen C et al (2016) DDB2 (damaged-DNA binding 2) protein: a new modulator of nanomechanical properties and cell adhesion of breast cancer cells. Nanoscale 8: 5268-5279

8. Huang J, Liu S, Chen Z et al (2016) Distinguishing cancerous liver cells using surface-enhanced raman spectroscopy. Technol Cancer Res T 15: 36-43

9. Abdolahad M, Janmaleki M, Taghinejad M et al (2013) Single-cell resolution diagnosis of cancer cells by carbon nanotube electrical spectroscopy. Nanoscale 5: 3421-3427

10. Hou HW, Li QS, Lee GY et al (2009) Deformability study of breast cancer cells using microfluidics. Biomed Microdevices 11: 557-564

11. Qu X, Zhang H, Chen H et al (2017) Convection driven pull-down assays in nanoliter droplets using scaffolded aptamers. Anal Chem 89:3468-3473

12. Ye Z, Li N, Zhao LB et al (2016) Super-resolution imaging and tracking of TGF-β receptor on living cells. Sci Bull 61: 632-638

13. Huang YQ, Yao X, Zhang R et al (2014) Cationic conjugated polymer/fluoresceinamine-hyaluronan complex for sensitive fluorescence detection of CD44 and tumor-targeted cell imaging. ACS App Mater Inter 6: 19144-19153

14. Speight RE, Cooper MA (2012) A survey of the 2010 quartz crystal microbalance literature. J Mol Recognit 25: 451-473

15. Abi A, Lin MH, Pei H et al (2014) Electrochemical switching with 3D DNA tetrahedral nanostructures self-assembled at gold electrodes. ACS App Mater Inter 6: 8928-8931

16. Zeng X, Shen Z, Mernaugh R (2012) Recombinant antibodies and their use in biosensors. Anal Bioanal Chem 402: 3027-3038

17. Zhang S, Bai H, Yang P (2015) Real-time monitoring of mechanical changes during dynamic adhesion of erythrocytes to endothelial cells by QCM-D. Chem Commun 51: 11449-11451

18. Tymchenko N, Nileback E, Voinova MV et al (2012) Reversible changes in cell morphology due to cytoskeletal rearrangements measured in real-time by QCM-D. Biointerphases 7: 43

19. Sha X, Sun C, Xu X et al (2012) Quartz crystal microbalance (QCM): useful for developing procedures for immobilization of proteins on solid surfaces. Anal Chem 84: 10298-10305

20. Yuan YJ, Chen QY, Li J (2016) QCM-based immunosensor for determining immunoglobulin g. RSC Adv 6: 40336-40342

21. Pei H, Zuo XL, Zhu D et al (2014) Functional DNA nanostructures for theranostic applications. Acc Chem Res 47: 550-559

22. Pan YL, Guo ML, Nie Z et al (2010) Selective collection and detection of leukemia cells on a magnet-quartz crystal microbalance system using aptamer-conjugated magnetic beads. Biosens Bioelectron 25: 1609-1614

23. Pei Z, Saint-Guirons J, Kack C et al (2012) Real-time analysis of the carbohydrates on cell surfaces using a QCM biosensor: a lectin-based approach. Biosens Bioelectron 35: 200-205

24. Braunhut SJ, McIntosh D, Vorotnikova E et al (2005) Detection of apoptosis and drug resistance of human breast cancer cells to taxane treatments using quartz crystal microbalance biosensor technology. Assay Drug Dev Technol 3: 77-88

25. Zhou T, Marx KA, Dewilde AH et al (2012) Dynamic cell adhesion and viscoelastic signatures distinguish normal from malignant human mammary cells using quartz crystal microbalance. Anal Biochem 421: 164-171

26. Tarantola M, Marel AK, Sunnick E et al (2010) Dynamics of human cancer cell lines monitored by electrical and acoustic fluctuation analysis. Integ Biol 2: 139-150

27. Zhang S, Bai H, Pi J et al (2015) Label-free quartz crystal microbalance with dissipation monitoring of resveratrol effect on mechanical changes and folate receptor expression levels of living MCF-7 cells: a model for screening of drugs. Anal Chem 87: 4797-4805

28. Atay S, Pişkin K, Yılmaz F et al (2016) Quartz crystal microbalance based biosensors for detecting highly metastatic breast cancer cells via their transferrin receptors. Anal Methods 8:

153-161

29. Sobiepanek A, Milner-Krawczyk M, Lekka M et al (2017) AFM and QCM-D as tools for the distinction of melanoma cells with a different metastatic potential. Biosens Bioelectron. 93:274-281

30. Culty M, Shizari M, Thompson E W. et al (1994) Binding and degradation of hyaluronan by human breast cancer cell lines expressing different forms of CD44: correlation with lnvasive potential. J Cell Physiol 160: 275-286

31. Marhaba R, Zoller M (2004) CD44 in cancer progression: Adhesion, migration and growth regulation. J Mol Histol 35: 211-231

32. Cho SH, Park YS, Kim HJ et al (2012) CD44 enhances the epithelial-mesenchymal transition in association with colon cancer invasion. Int J Oncol 41: 211-218

33. Montgomery N, Hill A, McFarlane S et al (2012) CD44 enhances invasion of basal-like breast cancer cells by upregulating serine protease and collagen-degrading enzymatic expression and activity. Breast Cancer Res 14: R84

34. Basakran NS (2015) CD44 as a potential diagnostic tumor marker. Saudi Med J 36: 273-279

35. Yin H, Zhao F, Zhang D et al (2015) Hyaluronic acid conjugated beta-cyclodextrin-oligoethylenimine star polymer for CD44-targeted gene delivery. Int J Pharm 483: 169-179

36. Yan J, Yang L, Lin MF et al (2013) Polydopamine spheres as active templates for convenient synthesis of various nanostructures. Small 9: 596-603

37. Yang J, Niu L, Zhang Z et al (2015) Electrochemical behavior of a polydopamine nanofilm. Anal Lett 48: 2031-2039

38. Li M, Jia X, Chang CY et al (2014) Bioinspired fabrication of composite nanofiltration membrane based on the formation of DA/PEI layer followed by cross-linking. J Membr Sci 459: 62-71

39. Zhang S, Bai H, Luo J et al (2014) A recyclable chitosan-based QCM biosensor for sensitive and selective detection of breast cancer cells in real time. Analyst 139: 6259-6265